Journal of Reproduction and Development, Vol. 62, No 6, 2016

—Original Article—

Effects of whole genome duplication on cell size and gene expression in mouse embryonic stem cells

Hiroyuki IMAI[1)], Wataru FUJII[2)], Ken Takeshi KUSAKABE[1)], Yasuo KISO[1)] and Kiyoshi KANO[1)]

[1)]*Laboratory of Veterinary Anatomy and Embryology, The United Graduate School of Veterinary Science, Yamaguchi University, Yamaguchi 753-8515, Japan*

[2)]*Laboratory of Applied Genetics, Graduate School of Agricultural and Life Sciences, The University of Tokyo, Tokyo 113-8657, Japan*

Abstract. Alterations in ploidy tend to influence cell physiology, which in the long-term, contribute to species adaptation and evolution. Polyploid cells are observed under physiological conditions in the nerve and liver tissues, and in tumorigenic processes. Although tetraploid cells have been studied in mammalian cells, the basic characteristics and alterations caused by whole genome duplication are still poorly understood. The purpose of this study was to acquire basic knowledge about the effect of whole genome duplication on the cell cycle, cell size, and gene expression. Using flow cytometry, we demonstrate that cell cycle subpopulations in mouse tetraploid embryonic stem cells (TESCs) were similar to those in embryonic stem cells (ESCs). We performed smear preparations and flow cytometric analysis to identify cell size alterations. These indicated that the relative cell volume of TESCs was approximately 2.2–2.5 fold that of ESCs. We also investigated the effect of whole genome duplication on the expression of housekeeping and pluripotency marker genes using quantitative real-time PCR with external RNA. We found that the target transcripts were 2.2 times more abundant in TESCs than those in ESCs. This indicated that gene expression and cell volume increased in parallel. Our findings suggest the existence of a homeostatic mechanism controlling the cytoplasmic transcript levels in accordance with genome volume changes caused by whole genome duplication.

Key words: Embryonic stem cells, Polyploidy, Relative transcript levels, Tetraploid, Whole genome duplication

(**J. Reprod. Dev. 62:** 571–576, 2016)

Whole genome duplication has a marked impact on cell physiology and is of fundamental importance for evolution. The genome of the present-day living mammals has been suggested to retain traces of two whole genome duplication events [1] for which evidence has been reported [2, 3]. Genome duplication promotes the ability to adapt to environmental changes [4]. It has also been observed in tumor-forming processes; tetraploid cells have been observed in 37% of human tumors [5]. The appearance of genome-duplicated tetraploid cells has been linked to mutation or aberrant *p53* expression [6]. Somatic polyploid cells, including tetraploid cells, appear in some tissues such as the nerves and the liver, under regular physiological conditions [7, 8]. Although the mechanism by which tetraploid cells appear has been studied in detail [8, 9], their biological characteristics and physiological alterations are still poorly understood. This is due to the limited numbers of tetraploid cells and the difficulty in tracking genome duplication in mammalian cells *in vivo*.

Mouse embryonic stem cells (ESCs) established from a single blastocyst are pluripotent and retain the ability to form germ cells after being injected into a host blastocyst [10]. The homogeneity of ESCs presents advantages for studies in embryology and cell biology, such as those concerning signaling pathways [11, 12]. Mammalian tetraploid cells can be produced artificially by inhibiting cell division in diploid cells using microtubule polymerization-interfering compounds such as cytochalasin-B [13]. However, tetraploid cells generated with cytochalasin-B often display aneuploidy. Tetraploid cells obtained from tumors exhibit chromosomal deletions and amplifications [14]. Thus, tetraploid cells produced by either method are not suitable for physiological characterization in mammals. We have previously established mouse tetraploid embryonic stem cells (TESCs) from a single tetraploid blastocyst produced by electrofusion [15]. TESCs can be also created by transferring two somatic cell nuclei into an enucleated single-celled embryo using specific nuclear transfer techniques [16]. The karyotypes of TESCs are more homogeneous and do not present any aberration in cell division or chromosomal defects due to highly stable chromosomes [15]. However, the relative proliferation rate of TESC lines is significantly lower than that of ESC lines [15]. Thus, even though TESC lines were successfully created using an established method, differences in proliferation rates compared to those of ESCs persisted.

The purpose of this study was to identify the effect of whole genome duplication on the cell cycle, cell size, and gene expression by analyzing TESCs and ESCs at the single-cell level. Our results indicate that mammalian cells may harbor homeostatic mechanisms responsible for maintaining the cytoplasmic concentration of transcripts in line with changes in genome volume.

Received: July 11, 2016
Accepted: July 19, 2016
Published online in J-STAGE: August 29, 2016

Correspondence: K Kano (e-mail: kanokiyo@yamaguchi-u.ac.jp)

Table 1. Sequences of primer sets used in this study

Gene	Forward primer (5' → 3')	Reverse primer (5' → 3')	Product size (bp)	Amplification efficiency (%)
Gapdh	GTGCTGAGTATGTCGTGGAGTC	CATACTTGGCAGGTTTCTCCAG	357	105.9
Actb	GGCTGTATTCCCCTCCATCG	CCAGTTGGTAACAATGCCATGT	240	97.9
Nanog	TCCTTGCCAGGAAGCAGAAGATGC	CACTGGTTTTTCTGCCACCGCTTG	233	96.2
Oct3/4	GCATACGAGTTCTGCGGAGGGATG	GGACTCCTCGGGAGTTGGTTCCAC	207	99.9
Cdk1	AGGCCTCGTGATGCTTTCAAGTGC	ATCCTCGGGTCTTTGGCCTTCTCA	152	98.7
Ccnb1	ATTCCCTCGGTGGGATTCAAGTGC	TTCAAAGCACACCCCTGGAAGAGC	116	106.5

Materials and Methods

Mouse ESC culture

Establishment of ESCs and TESCs has been described previously [15]. ESCs and TESCs were seeded on mitomycin C-treated mouse embryonic fibroblasts (MEFs) in ESGRO complete serum-free medium (Merck Millipore, Billerica, MA, USA) supplemented with 20% KnockOut serum replacement (Life Technologies Japan, Tokyo, Japan), 100 μg/ml penicillin, and 50 μg/ml streptomycin. The medium was changed every two days. The cells were routinely passaged on mitomycin C-treated MEFs using phosphate-buffered saline (PBS)-EDTA-Trypsin (PET) solution.

Alkaline phosphatase (AP) staining

After fixation with Lillie's buffer solution, AP staining was performed on TESC and ESC colonies using an Alkaline Phosphatase Detection Kit (SCR004; Merck Millipore) according to the manufacturer's protocol.

Flow cytometry

After trypsinization with the PET solution, 1×10^6 ESCs or TESCs were washed in ice-cold PBS, fixed in 1.4 ml ice-cold 100% ethanol, and incubated for at least 1 h at 4°C. Following removal of ethanol by centrifugation, the cells were resuspended in 1 ml PBS containing 100 μg/ml RNase A, and incubated for 1 h at 23°C. Next, the cells were stained with 40 μl propidium iodide solution (40 μg/ml). Subsequently, the mixture was incubated for 5 min at 23°C and filtered through a 40-μm mesh filter (KyoshinRikoh, Tokyo, Japan), followed by analysis on a BD Accuri C6 Flow Cytometer (Becton, Dickinson and Company, Franklin Lakes, NJ, USA).

Giemsa and hematoxylin-eosin staining

Following trypsinization with the PET solution, cells were fixed in Carnoy's solution for 30 min and placed on microscope slides. After drying, the slides were stained with Giemsa stain and hematoxylin-eosin. Cell diameters were measured using ImageJ software (US National Institutes of Health, Bethesda, MD, USA).

Quantitative real-time PCR (qRT-PCR)

Total RNA was isolated from ESCs and TESCs using the ReliaPrep RNA Cell MiniPrep System (Promega, Madison, WI, USA). Following the manufacturer's protocol, 1.2×10^8 copies of external standard RNA (External Standard Kit (λ polyA) for qPCR; TaKaRa Bio, Shiga, Japan) were added to a lysate containing 2×10^5 cells. Total RNA was quantified using a spectrophotometer (ND-1000 Nanodrop; Thermo Fisher Scientific, Waltham, MA, USA) and cDNA was synthesized using the QuantiTect Reverse Transcription Kit (Qiagen KK, Tokyo, Japan). qRT-PCR was performed using the Power SYBR Green PCR Master Mix (Applied Biosystems, Waltham, MA, USA) and the StepOnePlus Real-time PCR System (Life Technologies Japan Corporation). The amplification protocol consisted of the following steps: 95°C for 10 min, 40 cycles of 95°C for 15 sec, and 60°C for 60 sec. Relative transcript levels were determined by normalization to the external standard gene, λ polyA. The sequences of the primer sets are shown in Table 1.

Statistical analysis

Student's *t*-test was used to detect significant differences between experimental groups. P-values < 0.05 were considered statistically significant.

Results

Cell cycle alterations caused by whole genome duplication

In this study, we used three previously established and characterized cell lines: control diploid ESCs, ESC#1, #2, and, #3; and tetraploid ESCs, TESC#1, #2 and, #3 [15]. TESC lines maintained their initial morphology and positive AP staining even after 25 passages (Fig. 1). To investigate the influence of whole genome duplication on cell proliferation, we used flow cytometry to compare the cell cycle subpopulations in ESCs and TESCs. No significant differences were detected between ESCs and TESCs in the G1, S, and G2/M phases (Fig. 2A, B).

Cell volume alterations caused by whole genome duplication

To characterize the alterations in cell volume caused by whole genome duplication, the relative size of subconfluent ESCs and TESCs was determined by flow cytometry (Fig. 3A, B). The estimated relative diameter of TESCs, derived from the forward scatter (FSC) values (Fig. 3A), was 1.36 fold greater than that of ESCs (Fig. 3B, Table 2). Assuming that ESCs were perfect spheres, the relative TESCs/ESCs cell area and volume ratios were 1.85 and 2.53, respectively (Table 3).

Furthermore, to verify the flow cytometry data, we used Giemsa and hematoxylin-eosin staining to measure the cell area in fixed cells (Fig. 4A). The actual cell area of TESCs was significantly larger than that of ESCs (Fig. 4B). Assuming that ESCs were perfect spheres, we calculated a relative TESCs /ESCs cell volume of 2.29 (Table 3).

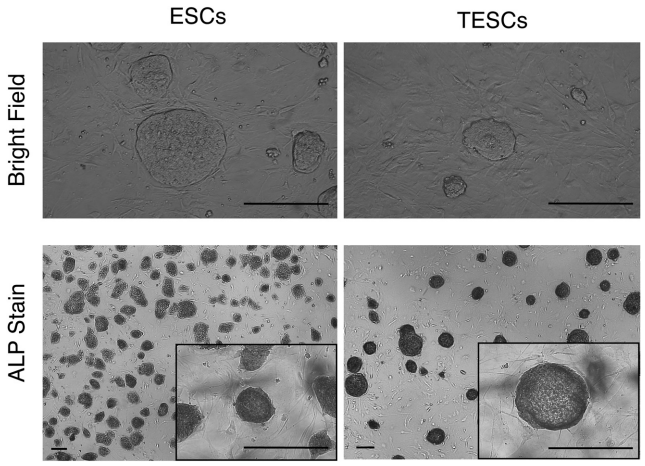

Fig. 1. Morphology of mouse tetraploid embryonic stem cells (TESCs) and mouse diploid embryonic stem cells (ESCs). Like ESCs, TESCs formed typical round-shaped colonies with clear boundaries. TESC colonies stained positive for the control ESC-positive marker alkaline phosphatase (AP). Representative images are shown. Scale bar, 50 μm.

Gene expression changes caused by whole genome duplication

To study the changes in gene expression caused by whole genome duplication we used qRT-PCR to measure the transcript levels in TESCs and ESCs. We used 2×10^5 cells/sample and known copy numbers of λ polyA RNA as the external standard (Fig. 5A). The relative gene expression level of the typical housekeeping genes, *Gapdh* and *Actb*, was significantly higher in TESCs than that in ESCs (2.15 and 2.27 fold, respectively) (Fig. 5B, Supplementary Fig. 1A: online only). In addition, the relative ratio of the cell cycle-associated genes, *Cdk1* and Cyclin B1 (*Ccnb1*) was generally higher in TESCs than that in ESCs (2.45 and 2.18 fold, respectively) (Supplementary Fig. 1B). We also analyzed two pluripotency markers, Nanog homeobox (*Nanog*) and Octamer-binding transcription factor 3/4 (*Oct3/4*), whose expression was 2.18 fold higher in TESCs than that in ESCs (Fig. 5C, Supplementary Fig. 1C), indicating a significantly higher level of absolute gene expression.

Discussion

In the present study, we investigated changes in the cell cycle, cell size, and gene expression caused by whole genome duplication in

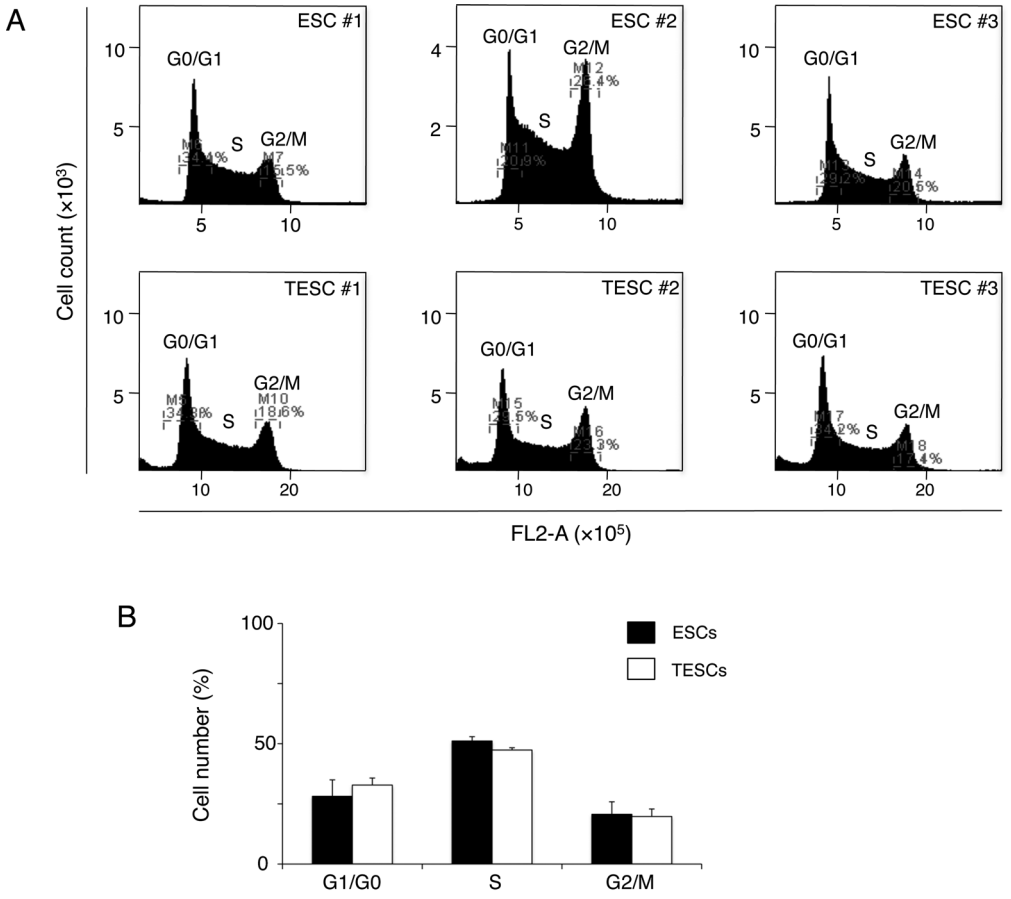

Fig. 2. Flow cytometric analysis of cell cycle distribution using propidium iodide staining. (A) Flow cytometry DNA histograms of different TESC and ESC lines. (B) Analysis of subpopulations in G1/G0, S, and G2/M phases. No significant differences were detected between the ESCs and TESCs for each phase. Data represent mean ± SD.

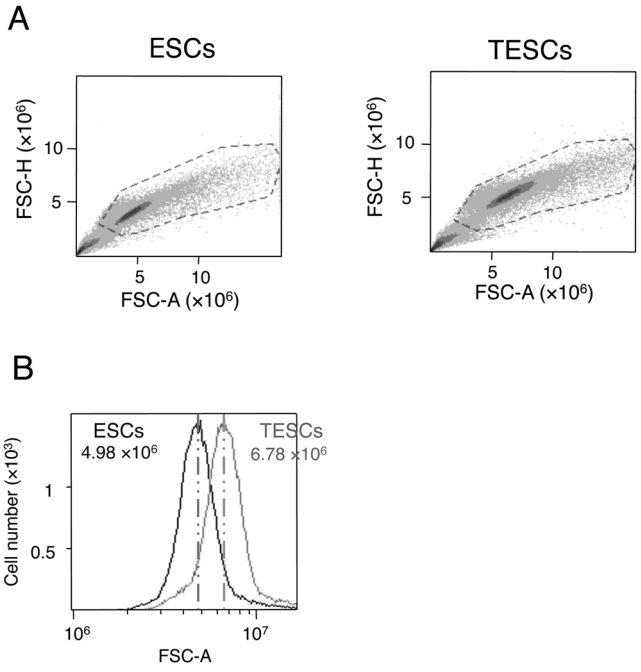

Fig. 3. Relative size measurement of TESCs and ESCs by flow cytometry. (A) Density plots of TESCs and ESCs stained with propidium iodide. (B) Debris-excluded histograms (FSC-A *vs*. cell number) for ESCs (blue) and TESCs (red). Average FSC values are shown. FSC = forward scatter.

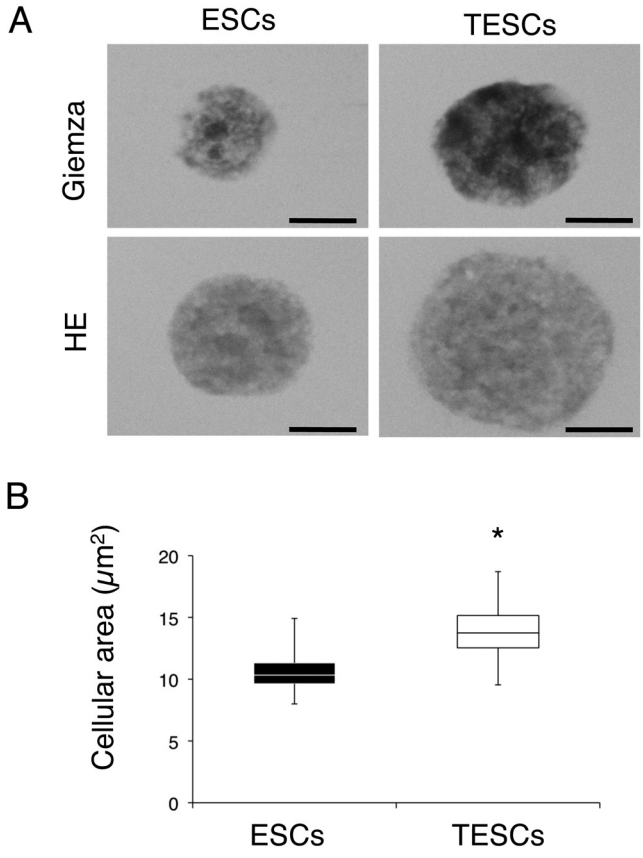

Fig. 4. Measurement of the cell area in fixed TESCs and ESCs. (A) Single ESCs and TESCs stained with Giemsa or hematoxylin-eosin (HE). Scale bar, 10 μm. Representative images are shown. (B) Cell area of single ESCs (n = 165) and TESCs (n = 135). Data represent mean ± SD. * $P < 0.05$.

Table 2. Relative ratio of cellular measurement in TESCs and ESCs

FSC (× 10^6)		Relative ratio (TESCs/ESCs)
ESCs	TESCs	
4.98 ± 0.07	6.78 ± 0.09	1.36

Table 3. Relative ratio of cellular measurement in TESCs and ESCs

Method	TESCs/ESCs		
	Diameter	Area	Volume
Flow cytometry	1.36	N.D.	2.53
Giemsa and H-E	N.D.	1.74	2.29

mouse TESCs. We found that TESCs maintained normal cell cycle progression and constant cytoplasmic transcript levels for housekeeping and pluripotency genes despite artificial tetraploidization. These results imply the existence of gene regulatory mechanisms that respond to changes in genome volume.

In this study, we employed TESCs as a novel model of polyploid cells to identify the biological features of polyploid cells arising from whole genome duplication. Tetraploid cells are known to exist in the nerve and liver tissues [7, 8], but they are scarce and are hence difficult to isolate and culture. Polyploidization, including whole genome duplication, is a frequent phenomenon in tumorigenesis. However, these polyploid cells are aneuploid, owing to chromosomal deletions or amplification, and the resulting cell populations are heterogeneous [17, 18]. In this context, TESCs are superior to tumor cell lines since they present a high degree of homology for each chromosome. Therefore, TESCs represent a novel model to analyze the impact of whole genome duplication on the fundamental features of mammalian cells.

We have previously shown that the relative proliferation rate of TESCs is significantly lower than that of ESCs [15]. The relative expression of cell cycle- and cell division-related genes is lower in mouse tetraploid blastocysts than that in mouse diploid blastocysts [19]. However, the relative mRNA concentration ratio of cell cycle associated genes, *Cdk1* and *Ccnb1*, did not differ significantly between TESCs and ESCs (Supplementary Fig. 1B). Thus, the lower proliferation rate of TESCs could not be attributed to alterations in cell cycle-related gene expression or to differences in the composition of the cell cycle subpopulation. Instead, it may depend on the prolonged duration of each cell cycle in TESCs due to the doubled genome volume due to tetraploidization. In the tetraploid cells produced from non-tumor diploid cells, such as fibroblasts, check points fail to trigger cell cycle arrest [20]. Here, we report that the cell cycle

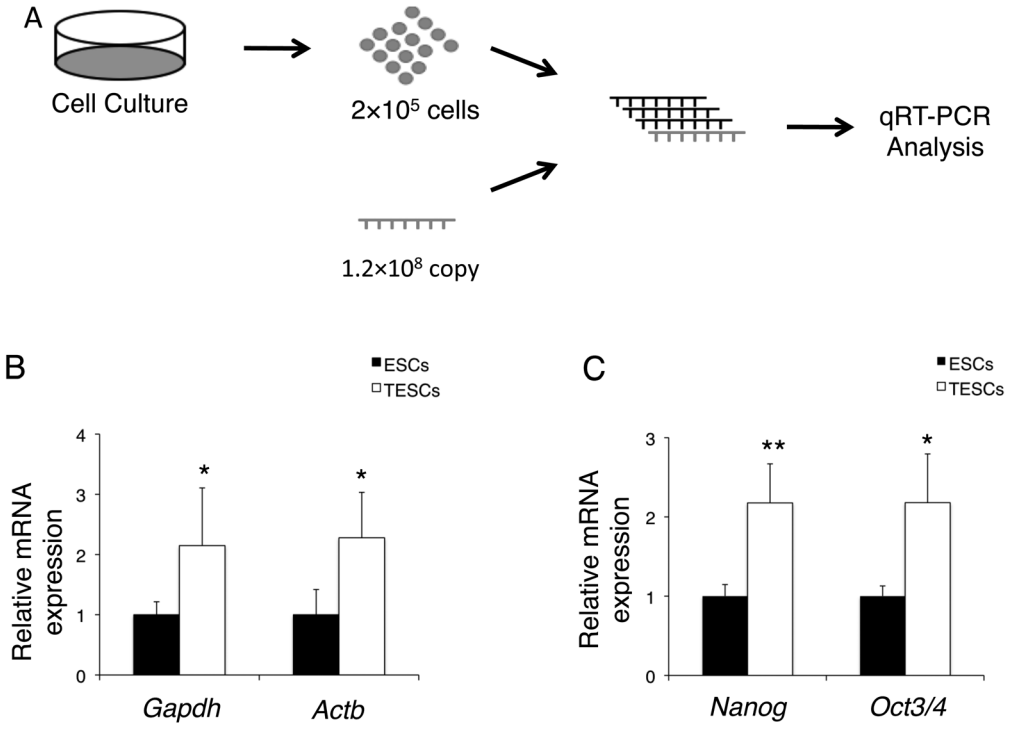

Fig. 5. Relative gene expression in TESCs and ESCs. (A) Schematic representation of gene expression analysis. Total RNA was extracted from 2×10^5 TESCs or ESCs and 1.2×10^8 copies of λ polyA RNA were added as external standard. Reverse transcription and quantitative real-time PCR (qRT-PCR) were performed. (B) Relative expression levels of housekeeping genes, *Gapdh* and *Actb*. (C) Relative expression levels of pluripotency marker genes, *Nanog* and *Oct3/4*. Data represent the mean ± SD (n = 6). * $P < 0.05$, ** $P < 0.01$.

subpopulations in TESCs do not differ substantially from those in ESCs, as observed by flow cytometric analysis, suggesting that cell cycle progression is not affected by whole genome duplication in mammalian cells.

To accurately identify the cell size alterations caused by whole genome duplication at the single-cell level, flow cytometric analysis was performed and actual cell size was measured by smear preparations. Accordingly, the calculated relative TESCs/ESCs cell volume ratio was found to be approximately 2.2–2.5-fold, suggesting that the mammalian cell volume doubles upon whole genome duplication.

Next, we investigated the effect of whole genome duplication on gene expression. Given that qRT-PCR is not suitable for measuring absolute expression levels, we employed a new method involving the addition of external RNA to a lysate containing 2×10^5 cells, and then performed the qRT-PCR [21]. Results revealed that the expression of the most common housekeeping genes in mouse ESCs, *Gapdh* and *Actb* [22, 23], was 2.2 fold higher in TESCs compared to that in ESCs. Although some reports have described the stable expression of *Gapdh* and *Actb* in mammalian embryos and in cultured cells, other studies have concluded that *Actb* is not a stably expressed gene [24–26]. Our findings suggest that the alteration of these two housekeeping genes is stable and homeostatic in mammalian ESCs, even after whole genome duplication. We extended our analysis to the pluripotency markers, *Nanog* and *Oct3/4*. The expression of these was 2.2 fold higher in TESCs than that in ESCs. Thus, whole genome duplication in mammalian cells appears to elicit the same alteration in the transcript levels of both housekeeping and essential genes.

Based on our findings, whole genome duplication caused a 2.2–2.5-fold expansion in cell volume and a 2.2 fold increase in gene expression. Drawing on the present results, we predict that the relative transcript levels might be kept constant in the cytoplasm of single ESCs despite whole genome duplication.

In summary, a comparison of tetraploid and diploid ESCs showed that whole genome duplication did not affect progression through the cell cycle, but doubled the cell volume and the expression of representative housekeeping and pluripotency marker genes. Further studies are required to characterize the molecular signals implicated in genome volume alteration in mammalian cells and their effects on genome dosage competition.

Acknowledgments

This study was supported in part by Grants-in-aid from the JSPS for Challenging Exploratory Research (24658237) to KK, for Young Scientists (A) (26712025) to WF, and for Scientific Research (B) (24380159) to YK. Additionally, Grants-in-Aid from The Foundation for Growth Science were awarded to KK.

References

1. **Ohno S.** Evolution by gene duplication. Berlin: Springer-Verlag; 1970.
2. **Panopoulou G, Poustka AJ.** Timing and mechanism of ancient vertebrate genome duplications — the adventure of a hypothesis. *Trends Genet* 2005; **21**: 559–567. [Medline] [CrossRef]
3. **Kasahara M.** The 2R hypothesis: an update. *Curr Opin Immunol* 2007; **19**: 547–552. [Medline] [CrossRef]
4. **Brodsky VY, Uryvaeva IV.** Genome multiplication in growth and development: biology of polyploid and polytene cells. London: Cambridge University Press; 1985.
5. **Zack TI, Schumacher SE, Carter SL, Cherniack AD, Saksena G, Tabak B, Lawrence MS, Zhsng CZ, Wala J, Mermel CH, Sougnez C, Gabriel SB, Hernandez B, Shen H, Laird PW, Getz G, Meyerson M, Beroukhim R.** Pan-cancer patterns of somatic copy number alteration. *Nat Genet* 2013; **45**: 1134–1140. [Medline] [CrossRef]
6. **Davaadelger B, Shen H, Maki CG.** Novel roles for p53 in the genesis and targeting of tetraploid cancer cells. *PLoS ONE* 2014; **9**: e110844. [Medline] [CrossRef]
7. **Morillo SM, Abanto EP, Román MJ, Frade JM.** Nerve growth factor-induced cell cycle reentry in newborn neurons is triggered by $p38^{MAPK}$-dependent E2F4 phosphorylation. *Mol Cell Biol* 2012; **32**: 2722–2737. [Medline] [CrossRef]
8. **López-Sánchez N, Frade JM.** Genetic evidence for $p75^{NTR}$-dependent tetraploidy in cortical projection neurons from adult mice. *J Neurosci* 2013; **33**: 7488–7500. [Medline] [CrossRef]
9. **Tanaka H, Goto H, Inoko A, Makihara H, Enomoto A, Horimoto K, Matsuyama M, Kurita K, Izawa I, Inagaki M.** Cytokinetic failure-induced tetraploidy develops into aneuploidy, triggering skin aging in phosphovimentin-deficient mice. *J Biol Chem* 2015; **290**: 12984–12998. [Medline] [CrossRef]
10. **Evans MJ, Kaufman MH.** Establishment in culture of pluripotential cells from mouse embryos. *Nature* 1981; **292**: 154–156. [Medline] [CrossRef]
11. **Kawazoe S, Ikeda N, Miki K, Shibuya M, Morikawa K, Nakano S, Oshimura M, Hisatome I, Shirayoshi Y.** Extrinsic factors derived from mouse embryonal carcinoma cell lines maintain pluripotency of mouse embryonic stem cells through a novel signal pathway. *Dev Growth Differ* 2009; **51**: 81–93. [Medline] [CrossRef]
12. **Abu Dawud R, Schreiber K, Schomburg D, Adjaye J.** Human embryonic stem cells and embryonal carcinoma cells have overlapping and distinct metabolic signatures. *PLoS ONE* 2012; **7**: e39896. [Medline] [CrossRef]
13. **Hoehn H, Sprague CA, Martin GM.** Effects of cytochalasin B on cultivated human diploid fibroblasts and its use for the isolation of tetraploid clones. *Exp Cell Res* 1973; **76**: 170–174. [Medline] [CrossRef]
14. **Gundimeda SD, Ahmed F, Mundada MC, Rajappa SJ, Murthy SS.** A near tetraploid clone in acute myeloid leukemia with CD56 expression. *J Cancer Res Ther* 2014; **10**: 187–190. [Medline] [CrossRef]
15. **Imai H, Kano K, Fujii W, Takasawa K, Wakitani S, Hiyama M, Nishino K, Kusakabe KT, Kiso Y.** Tetraploid Embryonic Stem Cells Maintain Pluripotency and Differentiation Potency into Three Germ Layers. *PLoS ONE* 2015; **10**: e0130585. [Medline] [CrossRef]
16. **Horii T, Yamamoto M, Morita S, Kimura M, Nagao Y, Hatada I.** p53 suppresses tetraploid development in mice. *Sci Rep* 2015; **5**: 8907. [Medline] [CrossRef]
17. **Kotecki M, Reddy PS, Cochran BH.** Isolation and characterization of a near-haploid human cell line. *Exp Cell Res* 1999; **252**: 273–280. [Medline] [CrossRef]
18. **Zach S, Zeev A, Dunsky A, Goldbourt U, Shimony T, Goldsmith R, Netz Y.** Perceived body size versus healthy body size and physical activity among adolescents - Results of a national survey. *Eur J Sport Sci* 2013; **13**: 723–731. [Medline] [CrossRef]
19. **Kawaguchi J, Kano K, Naito K.** Expression profiling of tetraploid mouse embryos in the developmental stages using a cDNA microarray analysis. *J Reprod Dev* 2009; **55**: 670–675. [Medline] [CrossRef]
20. **Wong C, Stearns T.** Mammalian cells lack checkpoints for tetraploidy, aberrant centrosome number, and cytokinesis failure. *BMC Cell Biol* 2005; **6**: 6. [Medline] [CrossRef]
21. **Gilsbach R, Kouta M, Bönisch H, Brüss M.** Comparison of in vitro and in vivo reference genes for internal standardization of real-time PCR data. *Biotechniques* 2006; **40**: 173–177. [Medline] [CrossRef]
22. **Ito S, D'Alessio AC, Taranova OV, Hong K, Sowers LC, Zhang Y.** Role of Tet proteins in 5mC to 5hmC conversion, ES-cell self-renewal and inner cell mass specification. *Nature* 2010; **466**: 1129–1133. [Medline] [CrossRef]
23. **Morgani SM, Canham MA, Nichols J, Sharov AA, Migueles RP, Ko MS, Brickman JM.** Totipotent embryonic stem cells arise in ground-state culture conditions. *Cell Reports* 2013; **3**: 1945–1957. [Medline] [CrossRef]
24. **Mamo S, Gal AB, Bodo S, Dinnyes A.** Quantitative evaluation and selection of reference genes in mouse oocytes and embryos cultured in vivo and in vitro. *BMC Dev Biol* 2007; **7**: 14. [Medline] [CrossRef]
25. **Smits K, Goossens K, Van Soom A, Govaere J, Hoogewijs M, Vanhaesebrouck E, Galli C, Colleoni S, Vandesompele J, Peelman L.** Selection of reference genes for quantitative real-time PCR in equine *in vivo* and fresh and frozen-thawed *in vitro* blastocysts. *BMC Res Notes* 2009; **2**: 246. [Medline] [CrossRef]
26. **Lin P, Lan X, Chen F, Yang Y, Jin Y, Wang A.** Reference gene selection for real-time quantitative PCR analysis of the mouse uterus in the peri-implantation period. *PLoS ONE* 2013; **8**: e62462. [Medline] [CrossRef]